Turkish Journal of Electromechanicsand Energy
ISSN: 2547-975X
Vol:7, No:3, Page 92-99 (2022)
https://www.scienceliterature.com

Application of adaptive fuzzy logic controller to improve photovoltaic pumping system performances

D. Rekioua[1,*], S. Bensmail[1], T.Rekioua[1]

[1]*Laboratoire de Technologie Indstrielle et de l'information (LTII), Université de Bejaia, 06000 Bejaia, Algérie*

ARTICLE INFO

***Article Type*:**
Research Article

Article History:
Received: 8 October 2022
Revised: 11 December 2022
Accepted: 13 December 2022
Published: 31 December 2022

Editor of the Article:
M. E. Şahin

Keywords:
Photovoltaic, Water pumping system, Adaptive fuzzy logic control

ABSTRACT

This research presents an optimization for a photovoltaic pumping system with an adaptive fuzzy logic controller (AFLC). This maximization power point tracking (MPPT) approach is compared with the traditional control Perturb &Observ (P&O) to demonstrate its efficiency. After a sizing study, an application is made under two different days, to satisfy water consumption in Bejaia city. Different models can be used in photovoltaic-pumping system. In our case, we apply a model where the electrical power input of the motor-pump is directly function of the water flow output for various total heads. A simulation study under MATLAB/Simulink has been made using P&O and AFLC approaches. The outcomes demonstrate that applying the AFLC method, particularly for low changes of solar irradiation, improves the system pumping performance. Thus, the amount of power extracted is more and consequently the volume of the pumped flow has been rised. It is also noticed a gain in pumping time. The different results show the superiority of AFLC approach in terms of power, water flow and speed.

Cite this article: D. Rekioua, S. Bensmail, T. Rekioua, "Application of adaptive fuzzy logic controller to improve photovoltaic pumping system performances," *Turkish Journal of Electromechanics & Energy*, 7(3), pp.92-99, 2022.

1. INTRODUCTION

Solar energy, which is widely accessible and cost-free, is used in many applications such as electrification, and water pumping, but due to the solar irradiance variations, optimization power techniques are used to increase photovoltaic power [1-2]. Maximum power point tracking (MPPT) is applied to continuously boost the solar panel's production of power. Many different MPPTs are used for PV generators [3–14]. It can be classical methods which are divided into direct or indirect methods. The most popular are perturb & observe (P&O) [4, 5, 15-21]. The most used fuzzy logic control (FLC) [3, 6, 7, 18, 19], the adaptive fuzzy logic control (AFLC) [1, 3, 7], the artificial neural networks (ANN) [1, 7, 14, 16, 20]. The perturb and observe (P&O) strategy is the most employed to determine the MPP point for PV systems. The FLC optimizes the increment magnitude to obtain fast and fine tracking. This method is widely used because of its advantages and fast response and gives better performances than the P&O, but the controller depends on speed and power variations [3, 11-12]. The AFLC is primarily used to change the FLC duty cycle for dealing with various external factors [3, 13-14].

This study compares an advanced strategy (AFLC) with a classical approach (P&O) before applying the two approaches to a solar pumping system. In our case, the model applied uses the electrical power input of the motor pump directly function of the water flow output for various total heads. Finally, an application is made to provide a family with water for two different days in the Bejaia area made under two different days, to satisfy water consumption in Bejaia city. The two MPPT methods have been compared in a study. The AFLC method performance is demonstrated by simulation results that were achieved under solar irradiation variations. The most significant improvements are a gain in pumping time and an increase in power.

2. PROPOSED SYSTEM MODEL

A photovoltaic pumping system includes a pumping subsystem and a photovoltaic generator. The system investigated in this article is depicted in Figure 1. PV panels, a DC/DC and a DC/AC converter, an induction motor connected to a centrifugal pump, and a water tank make up this device. For the optimization, two MPPT techniques are used (P&O and AFLC).

2.1. Photovoltaic Array Modelling

The model based on one diode and the equivalent circuit is represented in Figure 2. The equivalent diagram of a photovoltaic cell includes a current generator that models the solar irradiance and a diode in parallel that models the PN junction [3].

**Correspondingauthor's e-mail::djamila.ziani@univ-bejaia.dz*

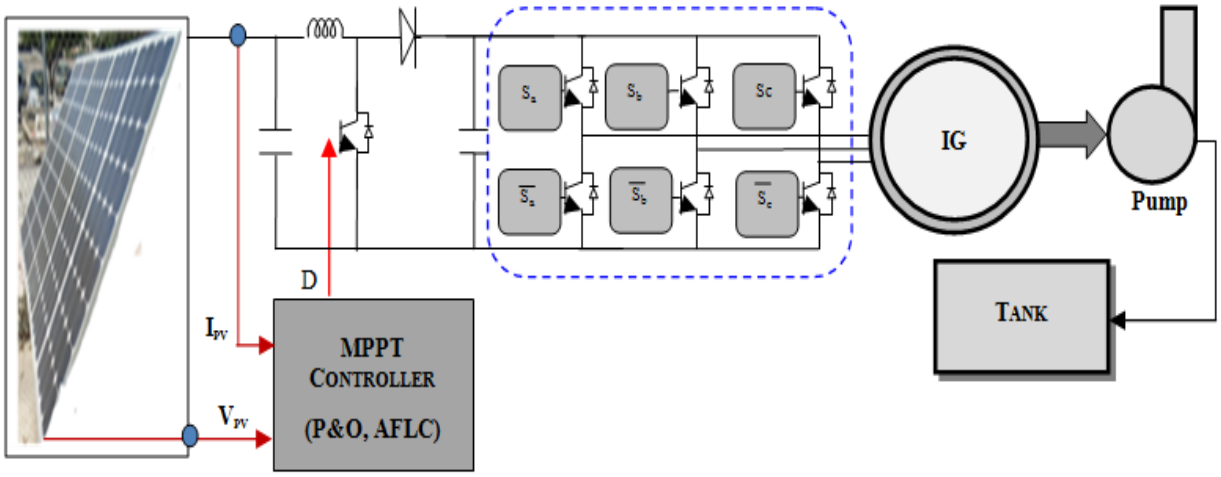

Fig.1. Studied photovoltaic pumping system.

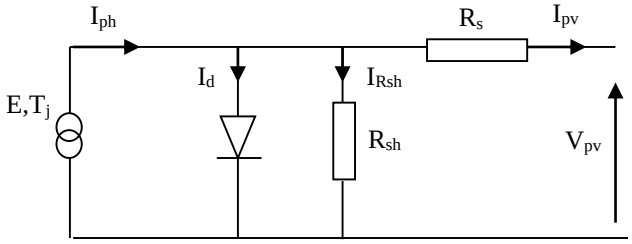

Fig. 2. One diode equivalent circuit.

Current characteristics are given by the following equation [5]:

$$I_{pv} = I_{ph} - I_0\left[e^{q\frac{(V_{pv}+I_{pv}.R_s)}{AkT_j}} - 1\right] - \frac{V_{pv}}{R_{sh}} \quad (1)$$

Where*: E* solar irradiation (W/m²), T_j junction temperature (°C), I_{ph} the photocurrent (A), I_d the junction polarization current (A), and R_s, R_{sh} are respectively serial and shunt resistances (Ω).

The used photovoltaic panels have the following characteristics as shown in Table 1.

Table.1 Parameter of the used PV panel.

Paramters	Values
P_{PV}	110Wp
I_{mpp}	3.15A
V_{mpp}	35V
I_{sc}	3.45A
V_{oc}	43.5V
α_{sc}	1.4mA/°C
β_{oc}	-152mV/°C
P_{mpp}	110W

Electrical characteristics are obtained by taking into account the effects of solar irradiance and temperature variations as shown in Figures 3, and 4.

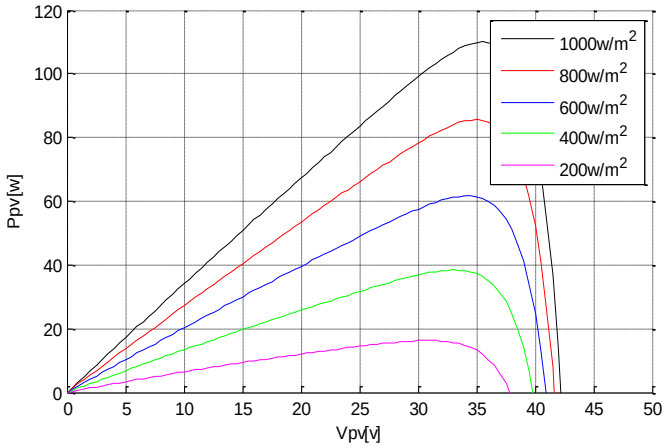

Fig. 3. Effects of solar irradiation variations on P_{pv}-I_{pv} characteristics.

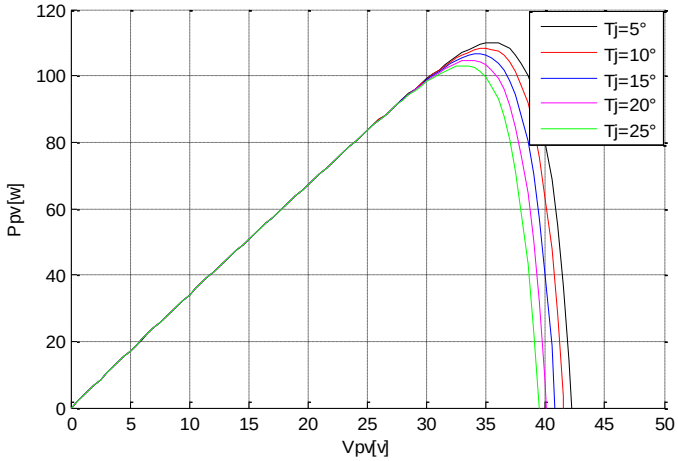

Fig. 4. Effects of temperature variations on P_{pv}-I_{pv}characteristics.

2.2. MPPT Algorithms

2.2.1. P&O algorithm

The most common approach is the P&O approach [2–12]. A deliberate panel voltage disturbance is made and the power obtained after the disturbance is compared with that power. In particular, when the power panel is increased as a result of the disturbance, the following disturbance will happen in the same direction. Additionally, a new disturbance is created in the opposite direction if the power decreases as shown in Figure 5. This approach is quite simple, knowing the characteristics of a solar generator is not necessary [8–11].

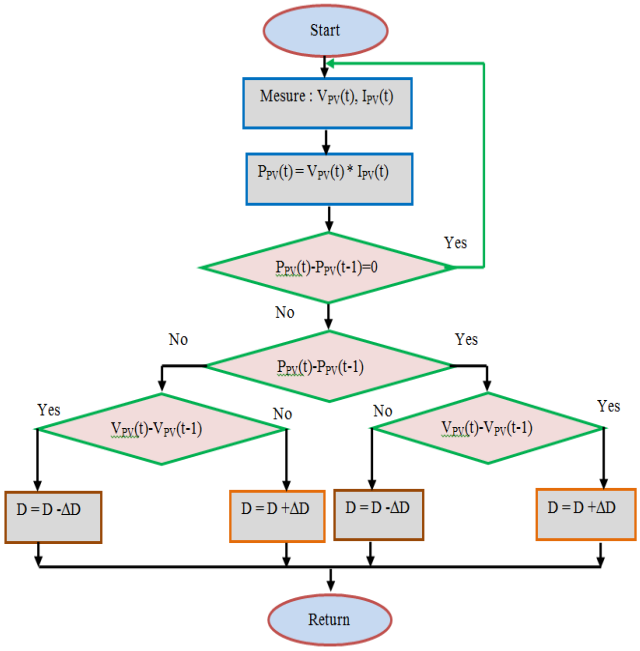

Fig. 5. P&O MPPT algorithm.

2.2.2. Adaptive fuzzy logic controller

The AFLC, which is an upgraded version of the FLC is primarily used to change the FLC duty cycle. The PV module's voltage and current are added to the preceding values to produce the average value. The structure of AFLC is given in Figure 6. As seen in the figure, the AFLC method is made up of two parts: a fuzzy basic learning controller and a learning mechanism. This one aims to study the environmental parameters and modify the FLC accordingly so that the global system response is close to the optimum point. As it is illustrated in Figure 6 the learning mechanism consists of an inverse fuzzy model and a modifier of the learning base.

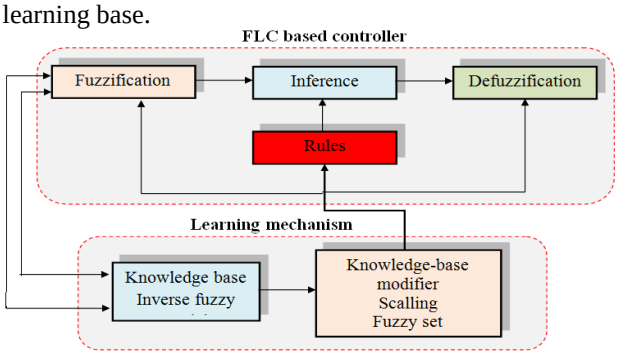

Fig. 6. AFLC structure.

The fuzzy parameters can be adapted using the following condition: If error < ε (limit value) then the learning basis modifier will be chosen. When a fuzzy variable's scaling factor is changed, each membership function's definition will be changed; therefore, changing any scaling factor can change the meaning of any rule. Any scaling factor can alter the meaning of any rule since it affects how each membership function is defined when a fuzzy variable's scaling factor is altered as shown in Table 2. Changing peak values can improve both speed and stability. A large error (NM and PM) can improve speed. While a small error (NS and PS) can improve stability. Rule base modification can affect the control system such as overshoot, catch time, and stability. When membership functions of a fuzzy set are changed, it may affect some rule bases. However, when a rule is changed, only that rule is involved.

Table 2. Fuzzy variable's scaling factor.

Converted fuzzy model		*The modified learning base*	
Error (e)	*Variation of error*	*Peak membership*	*Scaling factor*
$-\varepsilon\langle e(k)\langle\varepsilon$	$-\varepsilon\langle Ce(k)\langle\varepsilon$	$c(k)$	$e(k)=e(k)*\delta_3$
$e(k)\rangle\varepsilon$	$-\varepsilon\langle Ce(k)\langle\varepsilon$	$c(k)+\delta_2$	*Inchanged*
$e(k)\rangle\varepsilon$	$Ce(k)\rangle\varepsilon$	$c(k)+\delta_1$	*Inchanged*
$e(k)\rangle\varepsilon$	$Ce(k)\langle-\varepsilon$	$c(k)$	$e(k)=e(k)*\delta_3$
$e(k)\langle-\varepsilon$	$-\varepsilon\langle Ce(k)\langle\varepsilon$	$c(k)-\delta_2$	*Inchanged*
$e(k)\langle-\varepsilon$	$Ce(k)\rangle\varepsilon$	$c(k)$	$e(k)=e(k)*\delta_3$
$e(k)\langle-\varepsilon$	$Ce(k)\langle-\varepsilon$	$c(k)-\delta_1$	*Inchanged*

Where: ε is the minimum of the error, and $c(k)$ is the triangle peak of membership k.

The PV module's voltage and current are added to the preceding values to produce the average value. To alter the fuzzy parameters and improve system performance, the error and variation errors of the system are used [13-14].

$$e(k)=\frac{P_{pv}(k+1)-P_{pv}(k)}{V_{pv}(k+1)-V_{pv}(k)} \quad (2)$$

$$Ce(k)=e(k+1)-e(k) \quad (3)$$

Table 3 illustrates the controller Mamdani type with functions for membership in seven classes.

Table. 3. AFLC rules table.

Error (e)	*Variation error (Ce)*						
	NB	*NM*	*NS*	*ZE*	*PS*	*PM*	*PM*
NB	NB	NB	NM	ZE	ZE	ZE	ZE
NM	NB	NM	NM	ZE	NM	PS	PS
NS	NB	NB	NB	NB	PM	PS	PM
ZE	NB	NB	NS	ZE	PS	PM	PB
PS	NM	NS	ZE	PS	PM	PB	PB
PM	NS	PB	PB	PB	PB	PB	PB
PB	ZE	PB	PB	PB	PB	PB	PB

Both the fuzzy logic control and the adaptive mechanism make up the AFLC technique. The fuzzification, fuzzy rules, and defuzzification as shown in Figure 7 (a-c) are three separate parts that make up the FLC [14–15].

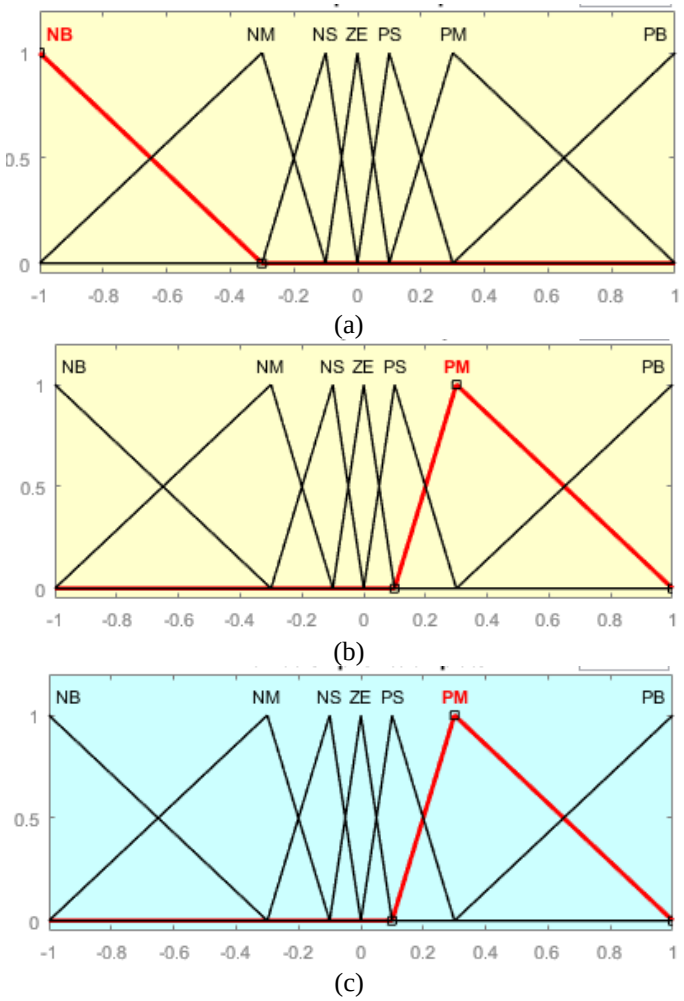

Fig. 7. AFLC membership functions, (a) Input variable *dP/dV*, (b) Input variable *DE*, (c) Output variable *Dd*.

2.3. Pumping Subsystem Model

2.3.1.Machine modelling

The induction motor mathematical model is described as follows [15]:

$$\begin{cases} V_{S\alpha} = R_{st} I_{S\alpha} + \dfrac{d\Phi_{S\alpha}}{dt} \\ V_{S\beta} = R_{st} I_{S\beta} + \dfrac{d\Phi_{S\beta}}{dt} \end{cases} \quad (4)$$

where: $I_{\sigma\alpha}$, *and* $I_{s\beta}$ are for α, β stator currents respectively (A), $\Phi_{s\alpha}$, $\Phi_{\sigma\beta}$ are for α, β stator flux respectively (Wb), and R_{st} is the stator resistance (Ω).

$$\begin{cases} 0 = V_{R\alpha} = R_R I_{R\alpha} + \dfrac{d\Phi_{R\alpha}}{dt} + \dfrac{d\theta}{dt}\Phi_{R\beta} \\ 0 = V_{R\beta} = R_R I_{R\beta} + \dfrac{d\Phi_{R\beta}}{dt} - \dfrac{d\theta}{dt}\Phi_{R\alpha} \end{cases} \quad (5)$$

where: $I_{R\alpha,} I_{R\beta}$ is for α, β rotor current respectively (A), $\Phi_{R\alpha}$, $\Phi_{R\beta}$ are for α, β rotor flux respectively (Wb), and R_r is the rotor resistance (Ω).

$$\begin{cases} \Phi_{S\alpha} = L_S I_{S\alpha} + L_m I_{R\alpha} \\ \Phi_{S\beta} = L_S I_{S\beta} + L_m I_{R\beta} \\ \Phi_{R\alpha} = L_R I_{R\alpha} + L_m I_{S\alpha} \\ \Phi_{R\beta} = L_R I_{R\beta} + L_m I_{S\beta} \end{cases} \quad (6)$$

Mechanical equations:

$$\begin{aligned} T_e - T_L &= J_m . \frac{d\omega_r}{dt} \\ T_e &= P \times (\phi_{s\alpha} \times I_{s\beta} - \phi_{s\beta} \times I_{s\alpha}) \end{aligned} \quad (7)$$

where T_e is the electromagnetic torque (N.m), T_L is the load torque (N.m), J_m is the inertia (N.m.s/rad), and P is the machine pole number.

2.3.2. Pumping system modelling

The PV-pumping system uses a wide range of different types of pumps. So, different models can be used. In our case, we apply a model where the electrical power input (P) to the motor pump is directly a function of the water flow output (Q) for various total heads. A polynomial fit of the third order is used [6, 7]:

$$P(Q,h) = a(h)Q^3 + b(h)Q^2 + c(h)Q + d(h) \quad (8)$$

Where a(h), b(h), c(h), and d(h) are the coefficients of the working total head.

$$a(h) = a_o + a_1 h^1 + a_2 h^2 + a_3 h^3 \quad (9)$$

$$b(h) = b_o + b_1 h^1 + b_2 h^2 + b_3 h^3 \quad (10)$$

$$c(h) = c_o + c_1 h^1 + c_2 h^2 + c_3 h^3 \quad (11)$$

$$d(h) = d_o + d_1 h^1 + d_2 h^2 + d_3 h^3 \quad (12)$$

With a_i, b_i, and d_i are solar pumping system constants (i=0, 1, 2, 3)

The Newton-Raphson method is used to compute the instantaneous flow in terms of power. The flow Q is therefore provided by the following equation at the k^{th} iteration:

For d – Pa (Q)> 0:

$$Q_k = Q_{k-1} - \frac{F(Q_{k-1})}{F'(Q_{k-1})} \quad (13)$$

With:

$$F(Q_{k-1}) = a Q^3_{k-1} + b Q^2_{k-1} + c Q_{k-1} + d - P_a(Q_{k-1}) \quad (14)$$

3. SIMULATION RESULTS

The P&O algorithm and the AFLC are compared in terms of maximum power point (MPP) tracking at various test conditions to demonstrate the proposed MPPT's robustness as shown in Table 4.

Table. 4. Different tests of solar irradiance and ambient temperature.

Tests	*E (W/m²)*	*T(°C)*
Test 1	1000	25
Test 2	600	30
Test 3	300	20

MATLAB/Simulink is used for simulation. The different obtained results for each test are shown in Figures 7-18. The two MPPT strategies (P&O and AFLC) were used to compare water flow, rotational speed, and electromagnetic torque in three different tests. We notice that the pump starts faster when using AFLC, which improves the speed and the electromagnetic torque. We can also have a good pump operation for very low irradiation values which is very interesting.

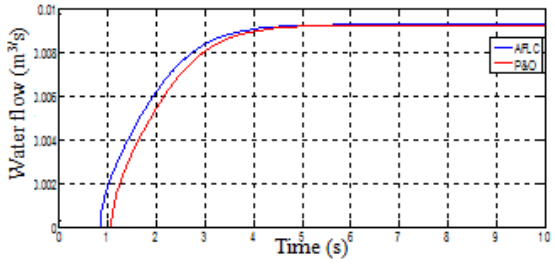

Fig. 7. Pump flow-Test-1.

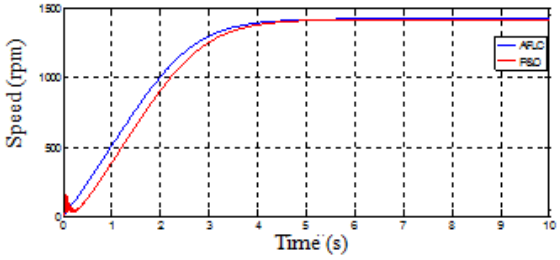

Fig. 8. Speed variations-Test-1.

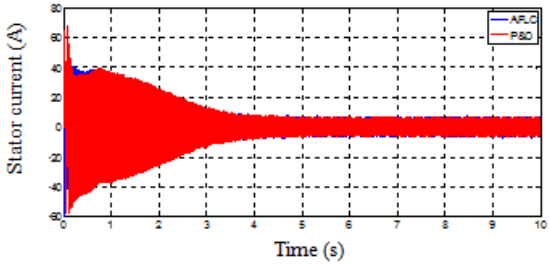

Fig. 9. Stator current-Test-1.

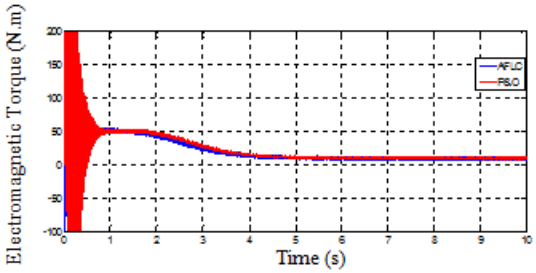

Fig. 10. Electromagnetic torque-Test-1.

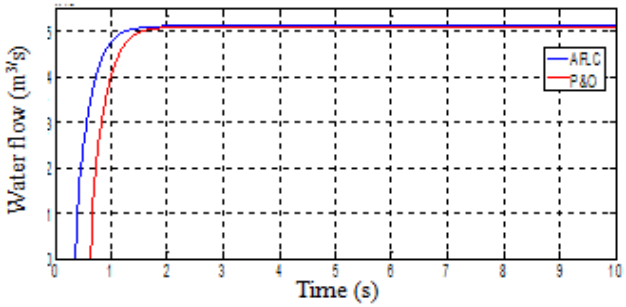

Fig.11. Pump flow at medium solar radiation- Test2

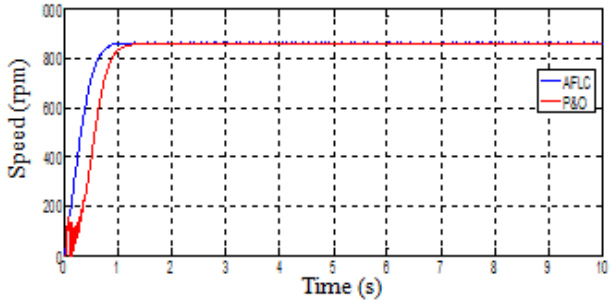

Fig. 12. Speed variations-Test-2.

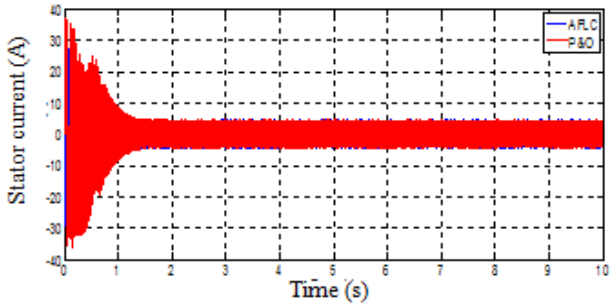

Fig. 13. Stator current –Test-2.

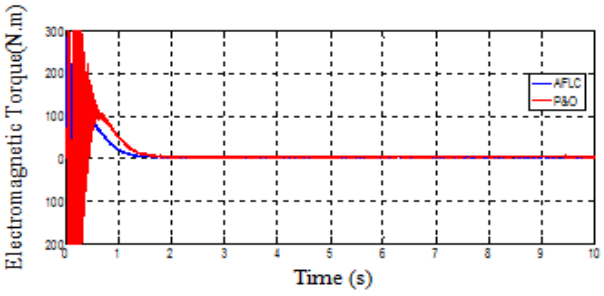

Fig. 14. Electromagnetic torque – Test-2.

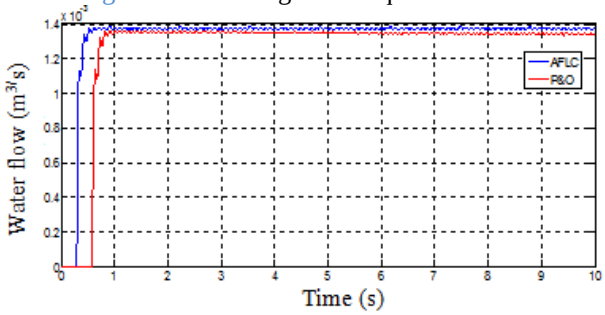

Fig. 15. Pump flow – Test-3.

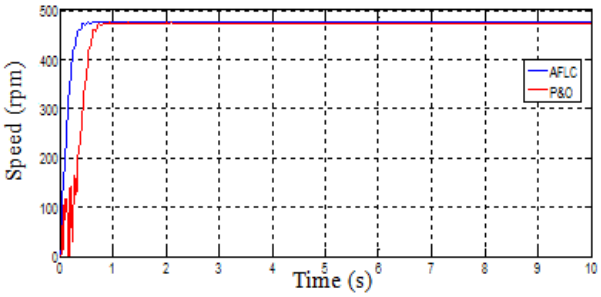

Fig. 16. Speed variations – Test-3.

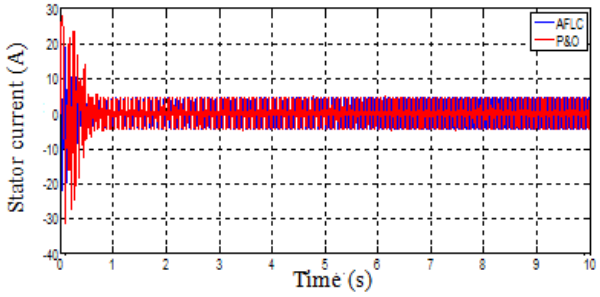

Fig. 17. Stator current – Test-3.

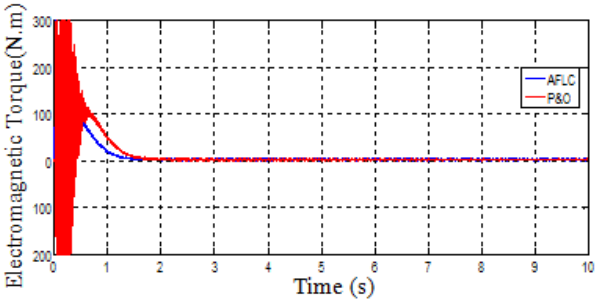

Fig. 18. Electromagnetic torque –Test-3.

When compared to the P&O approach, it is seen that the AFLC method responds more quickly whatever the different test conditions (low, medium, and high solar irradiations).

4. APPLICATION OF AFLC TO THE PUMPING SYSTEM

4.1.Sizing Photovoltaic Pumping System

The pumping system's sizing is carried out in two steps. The pumping sub-system must first be sized based on the flow rate, tank size, and dynamic total head. Then, an appropriate size of the PV generator must be determined based on whether conditions in the Bejaia area as in Figure.19.

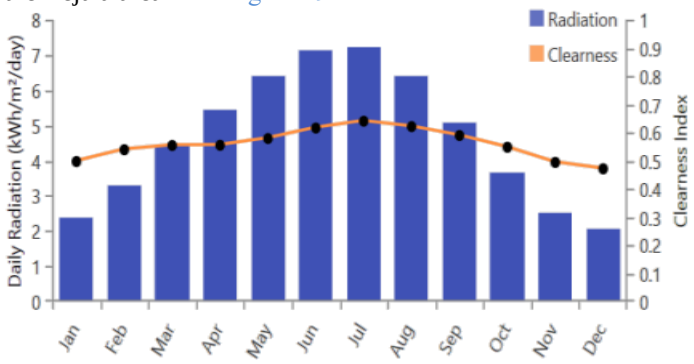

Fig. 19. Weather conditions in the Bejaia area.

The different equations used to calculate the PV energy are:

$$\begin{cases} P_{Hydro} = \rho.g.H.Q_v \\ P_{mec} = P_{Hydro}/\eta_{pump} \\ P_{elect} = P_{elec}/\eta_{IM} \\ P_{inv} = P_{elec}/\eta_{inv} \\ \tau_{pump} = V_{tank}/Q_v \\ E_{pv,m} = \tau_{pump}.P_{inv} \end{cases} \quad (15)$$

Where P_{hydro} is the hydropower (W), P_{mec} is the mechanical power (W), P_{elect} is the electrical power (W), P_{inv} is the inverter input power (W), τ_{pump} is the pumping time (hours/day), Q_v is the volumetric water flow (m^3/s), H is the dynamic level head (m), η_{pump}, η_{inv}, η_m are respectively the pump, inverter and motor efficiency (%), and $E_{pv,m}$ is the monthly photovoltaic energy (kWh/m^2).

4.2. Application

The photovoltaic pumping system's size has been determined. It comprises a 100 m^3 water tank to satisfy a family's domestic needs in the Bejaia area on two different days. The nominal flow rate is chosen to be 34 m^3/h=0.0094 m^3/s, while the dynamic level head measures approximately 10 meters. The obtained results are summarized in Table 5.

Table 5. Sizing results of the pumping system.

Parameters	*Results*
P_{Hydro}	926,50 W
P_{mec}	1684.5 W
P_{elec}	2105.62 W
P_{inv}	2477.20 W
τ_{pump}	2.94 hours/day
$E_{pv,m}$	9103.72 Wh/day
P_{pv}	3096.50 Wp

MATLAB/Simulink was used to carry out the simulation investigation and the photovoltaic power. The chosen profile solar irradiance is given in Figure 20 (a) and the flow pump's results with and without MPPT are provided respectively in Figures 20 (b) and 20 (c). The AFLC technique improves the system pumping operation particularly in low changes of solar irradiation, as seen by the increased pumped flow from 0.005 m^3/s to 0.006 m^3/s. As the speed increases the extracted power becomes more significant, and the pumped flow follows. The operation starts before 2.5 s and before 4.5 s (on a time axis of 24 s) for high and low irradiation.

The system's operation is improved by using the AFLC method compared to direct coupling, especially under low solar irradiation, such that the extracted power is higher so the speed increases which increases the pumped flow rate.

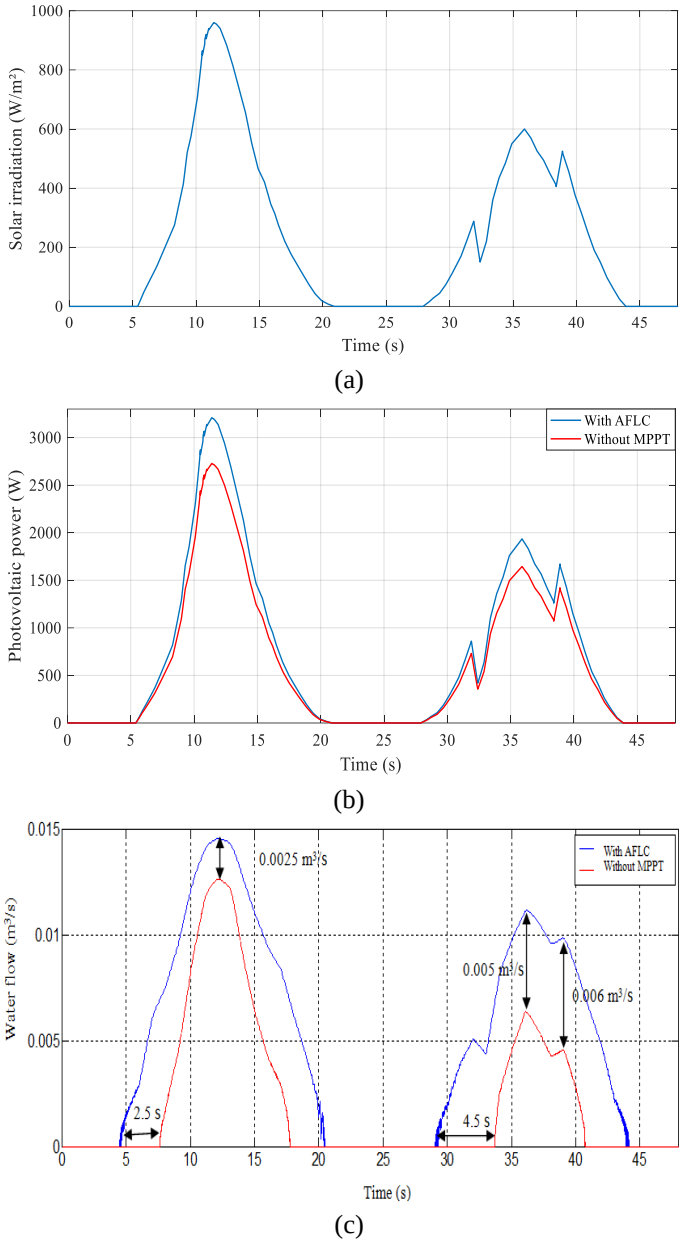

Fig. 20. (a) Solar irradiance variations during two days, (b) Photovoltaic power variations with and without MPPT, (c) Water flow pump variations with and without MPPT.

5. CONCLUSION

In this study, P&O and AFLC MPPT techniques used in solar pumping systems, have been compared. An application is made to satisfy a family's water needs in the Bejaia area. It has been observed that increased mechanical power caused by the AFLC results in increased water flow. This has improved the system pumping operation, particularly in low changes of solar irradiation, as seen by the increased pumped flow from 0.005 m^3/s to 0.006 m^3/s. As the speed increases the extracted power becomes more significant, and the pumped flow follows. The operation starts before 2.5 s and before 4.5 s (on a time axis of 24 s) for high and low irradiation. The control with the AFLC technique is superior in terms of power, water flow, and speed, according to the simulation results. It will be interesting in the future to compare the obtained simulation results to experimental ones.

Nomenclature

E	Solar irradiation (W/m²)
$E_{pv,m}$	Monthly photovoltaic energy (kWh/m²)
J_m	Inertia (N.m.s/rad)
I_{ph}	Light-generated current (A)
I_d	Diode current (A)
$I_{R\alpha}, I_{R\beta}$	α, β rotor current (A)
I_{Rsh}	Shunt-leakage current (A)
$I_{s\alpha}$, $I_{s\beta}$	α, β stator currents (A)
H	Dynamic level head (m)
P	Pole number
P_{ele}	Electrical power (W)
P_{hydro}	Hydropower (W)
P_{inv}	Inverter input power (W)
P_{mec}	Mechanical power (W)
R_s	Series resistance (Ω)
R_{sh}	Shunt resistance (Ω)
R_{st}	Stator resistance (Ω)
R_r	Rotor resistance (Ω)
T	Ambient temperature (°C)
T_e	Electromagnetic torque (N.m)
T_j	Junction temperature (°C)
T_L	Load torque (N.m)
Q_v	Volumetric water flow (m^3/s)
$\Phi_{s\alpha}$	α stator flux (Wb)
$\Phi_{\sigma\beta}$	β stator flux (Wb)
$\Phi_{R\alpha}$	α rotor flux (Wb)
$\Phi_{R\beta}$	β rotor flux (Wb)
ω_r	Rotor angular speed (rad/s)
τ_{pump}	Pumping time (hours/day)
η_{pump}	Pump efficiency (%)
η_{inv}	Inverter efficiency (%)
η_m	Motor efficiency (%)

References

[1] R. Akkaya, and A. A. Kulaksız, "A microcontroller-based stand-alone photovoltaic power system for residential appliances, " *Appl Energy*, 78(4), pp.419–431, 2004.

[2] C. Hua, Lin J, C. Shen, "Implementation of a DSP-controlled photovoltaic system with peak power tracking," *IEEE Trans Ind. Electron*., 45(1), pp.99–107, 1998.

[3] D. Rekioua, E. Matagne, "Optimization of photovoltaic power systems: Modelization, Simulation, and Control," *Green Energy and Technology*, vol. 102, pp.1-283, 2012.

[4] N. Femia, G. Petrone, G. Spagnuolo, "Optimization of Perturb and Observes Maximum Power Point Method Alignment," *IEEE Trans. on power electronics,"* 20(4), pp.963-973, 2005.

[5] V. Salas, E. Olias, A. Barrado, A. Làzaro, "Review of the maximum power point tracking algorithms for stand-alone photovoltaic systems," *Solar Energy Materials & Solar C*ells, 90(11), pp.1555–1578, 2006.

[6] S. Lalouni and D. Rekioua, "Modeling and simulation of a photovoltaic system using fuzzy logic controller," In Proceedings

of International Conference on Developments in eSystems Engineering, DeSE 2009, pp. 23–28, 2009.
[7] D. Rekioua, "MPPT Methods in Hybrid Renewable Energy Systems," *Green Energy and Technology*, pp. 79-138, 2020.
[8] R. Gules, J. Pellegrin Pacheco, HL. Hey, J. Imhoff, "A Maximum Power Point Tracking System with Parallel Connection for PV Stand-Alone Applications," *IEEE Transactions on Industrial Electronics*, 55(7), pp.2674–2683, 2008.
[9] D. P. Hohm, M. E. Ropp, "Comparative study of Maximum Power Point Tracking Algorithms," *Progress in Photovoltaics, Research and Applications*, 11(1), pp. 47-62, 2003.
[10] D. Sibtain, M. M. Gulzar, K. Shahid, I. Javed, S. Murawwat, M. M. Hussain, "Stability Analysis and Design of Variable Step-Size P&O Algorithm Based on Fuzzy Robust Tracking of MPPT for Standalone/Grid Connected Power System," *Sustainability (Switzerland)*, 14(15), art. no. 8986, 2022.
[11] T. Esram and P. L. Chapman, "Comparison of photovoltaic array maximum power point tracking techniques," *IEEE Trans. Energy Conversion*, 22(2), pp.439–449, 2007.
[12] D. Rekioua, S. Bensmail, N. Bettar, "Development of hybrid photovoltaic-fuel cell system for stand-alone application," *International Journal of Hydrogen Energy*, 39(3), pp. 1604-1611, 2014.
[13] M. B. Smida, A. Sakly, "Fuzzy logic control of a hybrid renewable energy system: A comparative study," *Wind Engineering*, 45(4), pp.793-806, 2021.
[14] M. I. S. Guerra, F. M. U. de Araujo, M. Dhimish, R. G. Vieira, "Assessing maximum power point tracking intelligent techniques on a PV system with a buck–boost converter," *Energies*, 14(22), art. no. 7453, 2021.
[15] A. Achour, D. Rekioua, A. Mohammedi, Z. Mokrani, T. Rekioua, S. Bacha, "Application of direct torque control to a photovoltaic pumping system with sliding-mode control optimization," *Electric Power Components and Systems*, 44(2), pp. 172-184, 2016.
[16] D. Rekioua, T. Rekioua, Y. Soufi, "Control of a grid-connected photovoltaic system," In *Proc. of the 2015 International Conference on Renewable Energy Research and Applications, ICRERA 2015*, art. no. 7418634, pp. 1382-1387, 2015.
[17] D.Rekioua, "Power Electronics in Hybrid Renewable Energies Systems," *Green Energy and Technology*, pp. 39-77, 2020.
[18] S. Lalouni, D. Rekioua, "Optimal control of a grid-connected photovoltaic system with the constant switching frequency," *Energy Procedia*, vol.36, pp. 189-199, 2013.
[19] A. Mohammedi, D. Rekioua, T. Rekioua, S. Bacha, "Valve Regulated Lead Acid battery behavior in a renewable energy system under an ideal Mediterranean climate," *International Journal of Hydrogen Energy*, 41(45), pp. 20928-20938, 2016.
[20] V. Pandurangan, P. Malik, "Supervisory control of operation of a cogeneration plant using fuzzy logic," *International Journal of Applied Power Engineering (IJAPE)*, 8(3), pp.234-248, 2016.
[21] D. Rekioua, A. Mohammedi, "Direct torque control for autonomous photovoltaic system with MPPT control," *Turkish Journal of Electromechanics & Energy*, 5(2), pp.48-55, 2020.
[22] D. Rekioua, F. Zaouche, H. Hassani, T. Rekioua, S. Bacha, "Modeling and fuzzy logic control of a stand-alone photovoltaic system with battery storage," *Turkish Journal of Electromechanics & Energy*, 4(1), pp.11-17, 2019.
[23] M. S. Ebrahim, A.M. Sharaf, A.M. Atallah, and A.S. Emarah, "An Efficient Controller for Standalone Hybrid-PV Powered System," *Turkish Journal of Electromechanics & Energy*, 2(1), pp.9-15, 2017.

Biographies

Djamila Rekioua is a professor at the University of Bejaïa. She obtained her Ph.D. in Electrical Engineering in 2002. She specializes in controlling electrical machines and renewable energies and has defended several Master's and Ph.D. theses. She has received several awards for her research work. Her main work focuses on wind, photovoltaic, fuel cells, storage, and multi-source systems. She is the author of several international publications and scientific papers. She is also a team leader and member of several research projects. In addition, she has published three books on photovoltaic systems (2012) and wind systems (2014), and hybrid renewable energy systems (2020) with Springer Editions. She is also responsible for training Master Renewable Energies and team leader of Renewable Energies and electro energy systems (ERSE) of the Excellency Laboratory of Research LTII (Laboratory of Industrial Technology and Information) of the University of Bejaia. She is a member of the LTII Laboratory.
E-mail: djamila.ziani@univ-bejaia.dz

Samia Bensmail obtained her doctorate in electrical engineering from the University of Bejaia (Algeria) in 2017 in the Electrical Engineering department. She has focused her study on a variety of subjects, including solar and wind systems, modeling, batteries, fuel cells, modelling and optimization, Fuzzy logic controllers, water pumping, and hybrid systems. She is a member of the LTII Laboratory.
E-mail: samia.bensmail@univ-bejaia.dz

Toufik Rekioua earned his engineering degree from the National Polytechnic Institute of Algiers, and in 1991, he received his doctorate from the I.N.P.L. of Nancy (France). Since 1992, he has served as a professor at the University of Bejaia's Electrical Engineering Department in Algeria. He is the author of several international publications and scientific papers. He is also a team leader and member of several research projects. His study focuses on solar, wind turbines, multi-source systems, power electronics and drives, electrical power engineering, renewable energies technologies, real-time, electric vehicles, Fuel cells, Supercapacities, batteries, and control in AC machines. He is the lead of the LTII laboratory
E-mail: toufik.rekioua@univ-bejaia.dz